Nonlinear Dynamics and Neuroscience

Izvestiya Vysshikh Uchebnykh Zavedeniy. Applied Nonlinear Dynamics. 2024;32(1)

Article DOI: 10.18500/0869-6632-003085

Synchronisation of the ensemble of nonidentical FitzHugh–Nagumo oscillators with memristive couplings

E. V. Navrotskaya, A. V. Kurbako, V. I. Ponomarenko, M. D. Prokhorov✉

Saratov Branch of Kotelnikov Institute of Radioengineering and Electronics of the RAS, Russia
E-mail: sidakev@gmail.com, kurbako.sasha@mail.ru, ponomarenkovi@gmail.com,
✉mdprokhorov@yandex.ru

Received 2.10.2023, accepted 15.11.2023, available online 28.12.2023, published 31.01.2024

Abstract. The *aim* of the study is to investigate the features of synchronization in ensembles of nonidentical neuron-like FitzHugh–Nagumo oscillators interacting via memristor-based coupling. *Methods.* The collective dynamics in a ring of FitzHugh–Nagumo oscillators connected via memristive coupling was studied numerically and experimentally. The nonidentity of oscillators was achieved by detuning them by the threshold parameter responsible for the excitation of oscillator, or by detuning them by the parameter characterizing the ratio of time scales, the value of which determines the natural frequency of oscillator. We investigated the synchronization of memristively coupled FitzHugh–Nagumo oscillators as a function of the magnitude of the coupling coefficient, the initial conditions of all variables, and the number of oscillators in the ensemble. As a measure of synchronization, we used a coefficient characterizing the closeness of oscillator trajectories. *Results.* It is shown that with memristive coupling of FitzHugh–Nagumo oscillators, their synchronization depends not only on the magnitude of the coupling coefficient, but also on the initial states of both the oscillators themselves and the variables responsible for the memristive coupling. We compared the synchronization features of nonidentical FitzHugh–Nagumo oscillators with memristive and diffusive couplings. It is shown that, in contrast to the case of diffusive coupling of oscillators, in the case of meristive coupling, with increasing coupling strength of the oscillators, the destruction of the regime of completely synchronous in-phase oscillations can be observed, instead of which a regime of out-of-phase oscillations appears. *Conclusion.* The obtained results can be used when solving the problems of synchronization control in ensembles of neuronlike oscillators, in particular, for achieving or destroying the regime of in-phase synchronization of oscillations in an ensemble of coupled oscillators.

Keywords: FitzHugh–Nagumo model, neuronlike oscillators, memristive coupling, radio physical experiment.

Acknowledgements. This study was supported by the Russian Science Foundation, Grant No. 22-22-00150, https://rscf.ru/project/22-22-00150/.

For citation: Navrotskaya EV, Kurbako AV, Ponomarenko VI, Prokhorov MD. Synchronisation of the ensemble of nonidentical FitzHugh–Nagumo oscillators with memristive couplings. Izvestiya VUZ. Applied Nonlinear Dynamics. 2024;32(1):96–110. DOI: 10.18500/0869-6632-003085

Introduction

Spiking neural networks, which use biologically realistic models of neurons as nodes, are the subject of intense study in various scientific disciplines [1]. Such networks are capable of demonstrating the activity inherent to real neurons, including generating spikes (pulses). Spiking neural networks are widely used to model information processing in the brain [2]. They are applied in classification and identification problems, for example, to classify typical patterns in biomedical signals (electroencephalograms, electromyograms, etc.) [3–6], classify external influences applied to network neurons [7, 8], and recognize audiovisual information [9, 10]. Spiking neural networks are of high practical importance in robotics when solving problems of robot motion control [11–14]. The development of new efficient algorithms for training spiking neural networks [15] opens up ever broader prospects for their practical application.

There are several well-known neuron models that are widely used as nodes for constructing spiking neural networks [16]. One of these models, which has become a reference model of excitable neuron dynamics, is the FitzHugh–Nagumo model [16]. Ensembles of coupled oscillators described by the FitzHugh–Nagumo equations have been studied by many authors. In particular, in such ensembles, the processes of formation, evolution, and synchronization of various spatio-temporal structures, including traveling waves and chimera states [17–21], were studied, and methods for controlling spatial structures using external influences [22, 23] were proposed.

The dynamics of spiking neural networks is determined not only by the choice of nodal elements of the network, but also by the choice of the type and structure of connections between neurons. When studying networks consisting of FitzHugh-Nagumo oscillators, the most widely used is the diffusive coupling, which models the electrical synaptic connection between neurons. Usually, in numerical modeling, such a coupling is assumed to be constant, independent of time. However, real neurons are characterized by the plasticity of synaptic connections, which ensures high adaptability of neural networks. The problem of implementing synaptic plasticity in spiking neural networks can be solved by using a memristive coupling between elements. A feature of such a coupling is the dependence of its value on the previous states of the interacting systems [24].

Neural ensembles and networks consisting of memristively coupled model neurons have been studied mainly numerically [25–28]. At the same time, spiking neural networks consisting of memristively coupled FitzHugh–Nagumo oscillators have been the subject of only a few studies. For example, in [29], the influence of initial states of memristive coupling on traveling waves in a ring of identical FitzHugh–Nagumo oscillators was studied. In [30], synchronization of two memristively coupled FitzHugh–Nagumo oscillators and a chain consisting of diffusion-coupled pairs of such oscillators was considered. The problem of experimental study of ensembles of memristively coupled FitzHugh–Nagumo oscillators is still poorly understood. For example, in the work [31] the synchronization of two neuron-like radio-technical generators of the FitzHugh-Nagumo type, connected via an analog memristive device, was experimentally studied.

In this paper, we numerically and experimentally investigated synchronization in an ensemble of memristively coupled non-identical FitzHugh-Nagumo oscillators. In a radiophysical experiment, we first implemented a network of 10 analog FitzHugh-Nagumo oscillators connected by a memristive coupling implemented in digital form.

1. Synchronization of two memristively coupled FitzHugh-Nagumo oscillators

Let us first consider two FitzHugh-Nagumo neuron-like oscillators, mutually connected by a memristive coupling and described by differential equations of the following form:

$$\begin{aligned} \varepsilon_i \dot{x}_i(t) &= x_i(t) - x_i^3(t)/3 - y_i(t) + kM(\varphi_i(t))(x_{i+1}(t) - x_i(t)), \\ \dot{y}_i(t) &= \gamma_i x_i(t) - y_i(t) + \beta, \\ \dot{\varphi}_i(t) &= x_i(t) - x_{i+1}(t), \end{aligned} \tag{1}$$

where $x_i(t)$ describes the dynamics of the membrane potential of the i-th neuron, $i = 1, 2$, with the boundary conditions $x_3(t) = x_1(t)$; $y_i(t)$ is responsible for restoring the membrane resting potential; $\varphi_i(t)$ determines the instantaneous state of the memristive coupling; ε_i is the parameter of the ratio of time scales, which is usually a small value; γ_i is the threshold parameter; the parameter β characterizes the conductivity of ion channels; k is the coupling coefficient; the function $M(\varphi_i(t)) = a + b\varphi_i^2(t)$ describes the conductivity of the i-th memristive coupling element, where a and b are the parameters of this function. This type of function describing memristive coupling was used in [24, 29, 30].

A memristor, a passive electrical element that can change its resistance depending on the electric charge passing through it, was first theoretically described by Chua [32]. Chua later developed the memristor concept and generalized it to any device whose characteristics depend on its operating history [33]. Such devices were called memristive [33]. Experimental examples of radio-technical devices with memristor properties appeared much later [34, 35].

The instantaneous value of the variable $\varphi_i(t)$ in the system (1) is determined as follows [29]:

$$\varphi_i(t) = \varphi_i(0) + \int_0^t (x_i(\tau) - x_{i+1}(\tau))\, d\tau. \tag{2}$$

The instantaneous value of the coupling strength of the oscillators in (1) depends on their previous states. Therefore, such coupling is interpreted as memristive.

We investigated the synchronization of oscillators in the (1) system depending on the magnitude of the coupling coefficient k and the initial conditions of all three variables: $x_i(0)$, $y_i(0)$, $\varphi_i(0)$. The non-identity of the oscillators was achieved by their detuning by the parameter γ_i or ε_i.

Let us consider the case of a small detuning of the oscillators in the parameter γ_i, which took the values $\gamma_1 = 1$ and $\gamma_2 = 1.05$, corresponding to periodic self-oscillations of uncoupled oscillators. The remaining parameters of the oscillators are the same: $\varepsilon_1 = \varepsilon_2 = 0.05$, $\beta = 0.2$. The parameters of the memristive coupling are $a = 1, b = 1$. In the numerical study of the (1) system, we integrated the model equations using the fourth-order Runge–Kutta method with a step of $\Delta t = 0.01$. To exclude the transient process, the time series of variables were not considered in the initial section of length $T_1 = 10000$.

As a measure of oscillator synchronization, we used the coefficient R, calculated using the following formulas [30]:

$$\begin{aligned} x_s &= (x_1 + x_2)/2, \\ R &= \frac{\langle x_s^2 \rangle - \langle x_s \rangle^2}{\frac{1}{2}\sum_{i=1}^{2}(\langle x_i^2 \rangle - \langle x_i \rangle^2)}, \end{aligned} \tag{3}$$

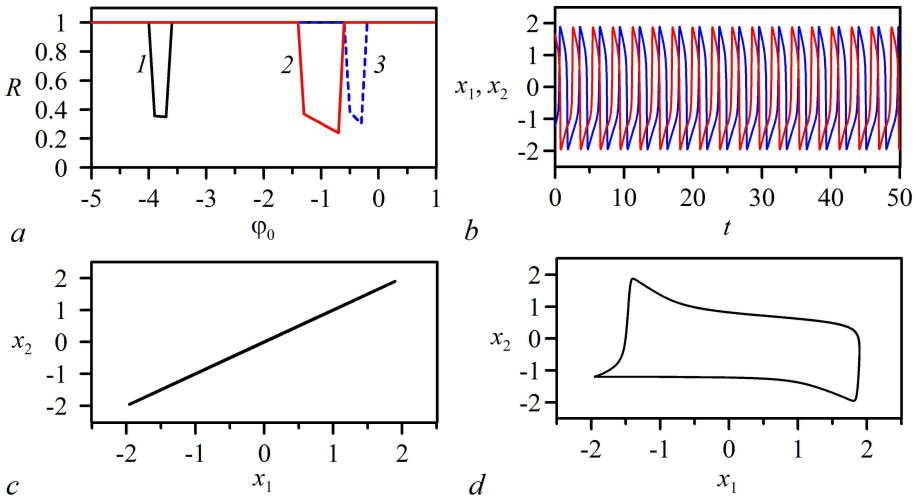

Fig 1. *a* — Dependences $R(\varphi_0)$ for $k = 0.0005$ (curve *1*), $k = 0.0025$ (curve *2*), and $k = 0.005$ (curve *3*) at $x_1(0) = x_2(0) = 0.2$, and $y_1(0) = y_2(0) = 0.1$. *b* — Temporal realizations of $x_1(t)$ and $x_2(t)$ at $\varphi_0 = -0.7$, $k = 0.0025$. *c* — Projection of oscillations in the case of in-phase mode at $\varphi_0 = -2$, $k = 0.0025$. *d* — Projection of oscillations in the case of out-of-phase mode at $\varphi_0 = -0.7$, $k = 0.0025$ (color online)

where the angle brackets denote averaging over time. For equal variances of the variables x_1 and x_2, the coefficient R is related to the mutual correlation coefficient r by the relation $R = (1 + r)/2$. The coefficient r can take values from -1 to 1. The coefficient R can vary from 0 to 1. For complete synchronization of the oscillators, the coefficient R is maximum and equals 1. In cases of asynchronous or out-of-phase oscillations of the oscillators, R takes small positive values [30]. To calculate R, we performed averaging over the time interval $T_2 = 1000$.

Let us denote $\varphi_1(0) = \varphi_2(0) = \varphi_0$ and plot the dependences $R(\varphi_0)$ for different values of k and $x_1(0) = x_2(0), y_1(0) = y_2(0)$ (Fig. 1, *a*). As can be seen from the figure, in a wide range of φ_0 values, the coefficient $R = 1$. This indicates complete synchronization of the oscillators. However, there is an interval of φ_0 values, in which the coefficient R is small. At higher values of the coupling coefficient ($k > 0.007$), the characteristic dip in the $R(\varphi_0)$ graph disappears and $R = 1$ for any values of φ_0.

Fig. 1, *b* shows the temporal realizations of the variables x_1 and x_2 for $\varphi_0 = -0.7$, $k = 0.0025$, at which the coefficient R takes a minimum value, $R = 0.24$. The variables $x_1(t)$ and $x_2(t)$ perform out-of-phase oscillations. In the range of values $R = 1$, the temporal realizations $x_1(t)$ and $x_2(t)$ almost coincide (not shown on the graph) and are practically indistinguishable, which indicates complete (in-phase) synchronization of the oscillators. Projections of the trajectory of

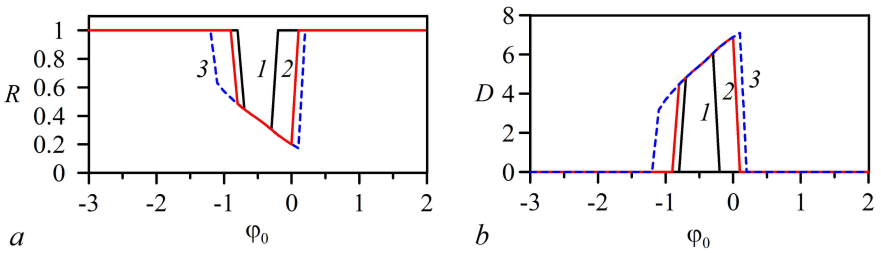

Fig 2. Dependences $R(\varphi_0)$ (*a*) and $D(\varphi_0)$ (*b*) for $k = 0.005$ and $x_1(0) = 0.2$, $x_2(0) = 0.4$, $y_1(0) = 0.1$, $y_2(0) = 0.3$ (curve *1*), $x_1(0) = 0.2$, $x_2(0) = 0.5$, $y_1(0) = 0.1$, $y_2(0) = 0.4$ (curve *2*), $x_1(0) = 0.2$, $x_2(0) = 2$, $y_1(0) = 0.1$, $y_2(0) = 1$ (curve *3*)

the system (1) on the plane (x_1, x_2) are given for the cases of in-phase ($R = 1$ (Fig. 1, *c*)), and out-of-phase ($R = 0.24$ (Fig. 1, *d*)) oscillations observed for different choices of initial conditions, $\varphi_0 = -2$ and $\varphi_0 = -0.7$, respectively. Due to the memristive coupling, non-identical oscillators are synchronized in frequency. In this case, they can be synchronized in phase (Fig. 1, *c*) or not synchronized in phase (Fig. 1, *d*).

The initial states of the variables $x_i(t)$ and $y_i(t)$ also affect the form of the dependencies $R(\varphi_0)$. In Fig. 2, *a* the graphs of $R(\varphi_0)$ are constructed for the cases $x_1(0) \neq x_2(0)$, $y_1(0) \neq y_2(0)$ at $k = 0.005$. It is evident that the more $x_1(0)$ differs from $x_2(0)$, and $y_1(0)$ from $y_2(0)$, the wider the region of absence of complete synchronization in the graph of $R(\varphi_0)$.

In addition to the R coefficient, we used another measure that characterizes the proximity of the trajectories of the first and second oscillators:

$$D = \frac{1}{L}\sum_{j=1}^{L}\Big((x_2(t_j) - x_1(t_j))^2 + (y_2(t_j) - y_1(t_j))^2\Big), \tag{4}$$

where j is the number of the time series point, L is the number of points. The closer the temporal realizations of the oscillators are to each other, the smaller the absolute value of D. When the oscillators are fully synchronized, $D = 0$.

In Fig. 2, *b* the dependences $D(\varphi_0)$ are constructed for the same cases as in Fig. 2, *a*, and $L = 100000$, corresponding to the same number of points as in the time interval $T_2 = 1000$ in Fig. 2, *a*. It is evident that there is a high correlation between the dependences $R(\varphi_0)$ and $D(\varphi_0)$: the dips in $R(\varphi_0)$ correspond to the rises in $D(\varphi_0)$ in the same ranges of φ_0 variation. Therefore, below we will use only the coefficient R as an illustration of the measure of oscillator synchronization.

Let us consider the dependence of the coefficient R on the value of the coupling coefficient k. Fig. 3, *a* shows the dependences $R(k)$, constructed for different values of φ_0. Starting from small positive values of k, the value of R reaches the maximum value $R = 1$. This indicates complete synchronization of the oscillators. However, with a further increase in k, the coefficient R decreases to small values. With an increase in the coupling strength of the oscillators, the destruction of the in-phase synchronization mode is observed. Instead, a mode of out-of-phase oscillations arises. Then, with an increase in k, the mode of complete (in-phase) synchronization of the oscillators is established again. For positive values of φ_0, the characteristic dip in the graph $R(k)$ disappears. $R = 1$ both for small and for high values of k.

The form of the graphs $R(k)$ depends not only on the initial conditions φ_0, but also on the initial conditions $x_i(0)$ and $y_i(0)$. In Fig. 3, *b* the graphs $R(k)$ are constructed for the cases $x_1(0) \neq x_2(0)$, $y_1(0) \neq y_2(0)$ with $\varphi_0 = -0.5$. Just as in the graphs $R(\varphi_0)$ in Fig. 2, *a*, the width

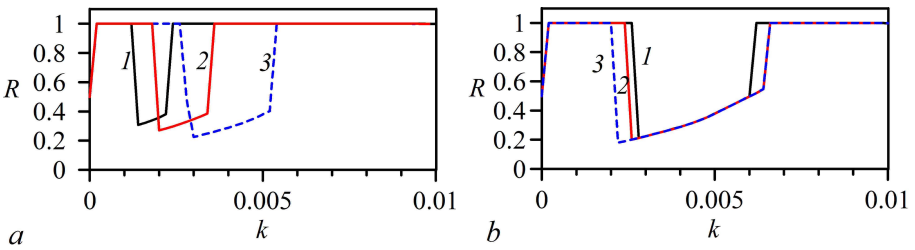

Fig 3. *a* — Dependences $R(k)$ for $\varphi_0 = -1.5$ (curve *1*), $\varphi_0 = -1$ (curve *2*), $\varphi_0 = -0.5$ (curve *3*) at $x_1(0) = x_2(0) = 0.2$, $y_1(0) = y_2(0) = 0.1$. *b* — Dependences $R(k)$ for $\varphi_0 = -0.5$ and $x_1(0) = 0.2$, $x_2(0) = 0.4$, $y_1(0) = 0.1$, $y_2(0) = 0.3$ (curve *1*), $x_1(0) = 0.2$, $x_2(0) = 1$, $y_1(0) = 0.1$, $y_2(0) = 0.5$ (curve *2*), $x_1(0) = 0.2$, $x_2(0) = 2$, $y_1(0) = 0.1$, $y_2(0) = 1$ (curve *3*)

of the region of small values of R in the graphs $R(k)$, corresponding to the absence of complete synchronization, increases with the growth of the difference between the values of $x_1(0)$ and $x_2(0)$, and $y_1(0)$ and $y_2(0)$ (Fig. 3, *b*).

Qualitatively similar results are obtained in the case of a small detuning of the oscillators by the parameter ε_i. The form of the dependences $R(\varphi_0)$ and $R(k)$ for $\varepsilon_1 \neq \varepsilon_2$ is similar to the above similar graphs for the detuning of the oscillators by the parameter γ_i.

Let us consider separately the case $b = 0$, corresponding to the diffusive coupling of the oscillators. In Fig. 4, *a* the dependence $R(k)$ is shown for the same parameter values as in Fig. 3, *a*, constructed for the memristive coupling. The value of R slowly monotonically increases with k, without demonstrating any dips. In Fig. 4, *b* the temporal realizations $x_1(t)$ and $x_2(t)$ for $k = 0.005$ are shown. In this case, the oscillators are not synchronized in frequency and demonstrate an asynchronous regime of two-frequency beats. The projection of the oscillations of the coupled system onto the plane (x_1, x_2) for this case is shown in Fig. 4, *c*. At $k = 0.1$ the oscillators are not yet completely synchronized, $R = 0.99$ (Fig. 4, *d*). In this case the oscillators demonstrate oscillations close to in-phase, having a very small phase shift. The projection of the system trajectory onto the plane (x_1, x_2) takes the form of a diagonal line only at $k = 2$ (with $R = 1$). This fully corresponds to synchronous in-phase oscillations. Thus, with diffusive coupling, higher values of the coupling coefficient k are required to synchronize non-identical oscillators.

In addition to numerical studies of the (1) model system, we conducted its experimental study. For this purpose, we used the ideology of analog modeling and constructed analog radio-technical generators of the FitzHugh–Nagumo type. Their dynamics are described by the first two equations of the (1) system at $k = 0$. To implement coupling between the generators, the National Instruments multichannel data input-output system was used. The block diagram of the experimental setup and its detailed description are given in [21]. In [21], a simple diffusive coupling between radio-technical generators was software-implemented, corresponding to the coupling of generators via a resistor. And in this work, memristive coupling of analog generators is implemented in digital form for the first time. Since the signals responsible for the coupling of generators are generated in the experimental setup software-based, it is quite easy to implement a time-varying mutual coupling of generators in it.

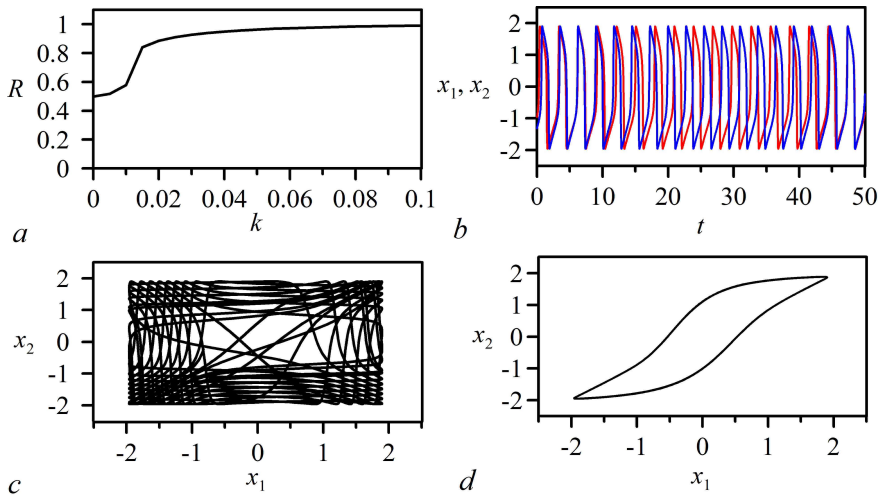

Fig 4. Case of diffusive coupling ($b = 0$). *a* — Dependence $R(k)$. *b* — Temporal realizations of $x_1(t)$ and $x_2(t)$ at $k = 0.005$. *c* — Projection of oscillations in the case of non-synchronous regime at $k = 0.005$. *d* — Projection of oscillations in the case of almost in-phase regime at $k = 0.1$ (color online)

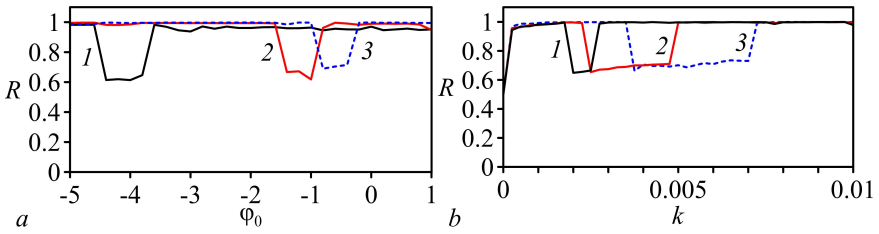

Fig 5. *a* — Experimental dependences $R(\varphi_0)$ for $k = 0.0005$ (curve *1*), $k = 0.0025$ (curve *2*), $k = 0.005$ (curve *3*). *b* — Experimental dependences $R(k)$ for $\varphi_0 = -1.5$ (curve *1*), $\varphi_0 = -1$ (curve *2*), $\varphi_0 = -0.5$ (curve *3*)

The experimentally obtained dependences $R(\varphi_0)$ are shown in Fig. 5, *a* for $\gamma_1 = 1$, $\gamma_2 = 1.05$, $\varepsilon_1 = \varepsilon_2 = 0.05$, $\beta = 0.2$, $a = 1$, $b = 1$ for three different values of k at $x_1(0) = x_2(0)$, $y_1(0) = y_2(0)$. The shape of these dependences is in qualitative agreement with the graphs $R(\varphi_0)$ constructed in Fig. 1, *a* in the numerical study of the system (1). Fig. 5, *b* shows the experimental dependences $R(k)$, constructed for different values of φ_0, which also agree well with the numerical results presented in Fig. 3, *a*.

2. Synchronization of oscillations in a ring of memristively coupled FitzHugh-Nagumo oscillators

Let us now consider an ensemble of FitzHugh-Nagumo oscillators, connected in a ring by a memristive coupling, described by model equations of the following form:

$$\begin{aligned} \varepsilon_i \dot{x}_i(t) &= x_i(t) - x_i^3(t)/3 - y_i(t) + k[M(\varphi_{i-1}(t))(x_{i-1}(t) - x_i(t)) + M(\varphi_i(t))(x_{i+1}(t) - x_i(t))], \\ \dot{y}_i(t) &= \gamma_i x_i(t) - y_i(t) + \beta, \\ \dot{\varphi}_i(t) &= x_i(t) - x_{i+1}(t), \end{aligned} \tag{5}$$

where, unlike the system (1), $i = 1, \ldots, N$, and the boundary conditions are $x_{i+N}(t) = x_N(t)$, where N is the number of oscillators. The form of the function $M(\varphi_i(t)) = a + b\varphi_i^2(t)$ is the same as in (1), with the same values of the parameters $a = 1$, $b = 1$. In the general case, all oscillators of the ensemble are non-identical.

As a measure of synchronization of oscillators, the coefficient R was used, calculated according to the following formulas [30]:

$$\begin{aligned} x_s &= \frac{1}{N}\sum_{i=1}^{N} x_i, \\ R &= \frac{\langle x_s^2\rangle - \langle x_s\rangle^2}{\frac{1}{N}\sum_{i=1}^{N}(\langle x_i^2\rangle - \langle x_i\rangle^2)}. \end{aligned} \tag{6}$$

As in the case of two oscillators (formula (3)), with complete synchronization of the oscillators, the coefficient R is maximum and equal to 1. In cases of asynchronous or out-of-phase oscillations of the oscillators, R takes small positive values [30]. For non-identical oscillators, at $k = 0$, the coefficient $R = 1/N$ and tends to zero at large N. To calculate R, we performed averaging over the time interval $T_2 = 1000$.

Let the oscillators be detuned by the parameter γ_i, the values of which are set randomly from the interval $[1, 1.05]$ and correspond to periodic self-oscillations of uncoupled oscillators. The other parameters of the oscillators are the same: $\varepsilon_i = 0.05$ for all i, $\beta = 0.2$. In Fig. 6, *a* the

dependence $R(k)$ is plotted for the case $N = 6$ with $\varphi_0 = -0.5$ and $x_i(0) = 0.2$, $y_i(0) = 0.1$ for all i. As in the case of two oscillators (Fig. 3), the dependence $R(k)$ in Fig. 6 has a characteristic range of k values, for which the coefficient R is relatively small. However, unlike Fig. 3, the region of small k values is clearly visible, at which R is relatively small and has not yet reached the value $R = 1$, corresponding to complete synchronization of the oscillators in the ensemble. This region of small k corresponds to asynchronous oscillations of the oscillators, as in the case shown in Fig. 4, *b*. The temporal realizations $x_i(t)$ of asynchronous oscillators are shown in Fig. 6, *b* for $k = 0.0001$.

Fig. 6, *c* shows the temporal realizations of $x_i(t)$ for $k = 0.002$ (with $R = 0.27$). In this case, the oscillators are synchronized in frequency, but demonstrate out-of-phase oscillations. There are two clusters in the ring, within which the oscillators oscillate almost in phase, and there is a phase shift between the clusters. For $k = 0.003$, the coefficient $R = 1$ and all oscillators are completely synchronized. Their temporal realizations practically coincide (Fig. 6, *d*).

When the number of non-identical oscillators in the ring becomes large enough, the shape of the $R(k)$ dependence changes. For example, at $N = 10$ it becomes strongly jagged in the region of small k values preceding the R coefficient reaching its maximum value (Fig. 7, *a*). This figure is constructed for the same parameters and initial states $x_i(0)$ and $y_i(0)$ as in Fig. 6, *a*. The jagged nature of the $R(k)$ dependence is explained by the fact that higher values of the coupling coefficient are required for complete synchronization of a large number of non-identical oscillators, while for small k cluster synchronization of oscillators can be observed.

In Fig. 7, *b* the dependence $R(\varphi_0)$ is plotted for $k = 0.001$ for a ring of 10 oscillators. Compared to the case of two oscillators (see Fig. 1, *a*), the dependence $R(\varphi_0)$ in Fig. 7, *b* has a very jagged appearance, and R is everywhere less than 1. This is explained by the absence of complete synchronization of the oscillators for any values of φ_0 for the chosen value of the coupling strength k.

We also considered cases when the initial states of the variables $x_i(t)$ and $y_i(t)$ of the oscillators in the chain differ. The initial conditions for $x_i(0)$ and $y_i(0)$ were set randomly in the ranges $[0.2, 2]$ and $[0.1, 1]$, respectively. In this case, the form of the dependencies $R(k)$ and $R(\varphi_0)$ changed. However, no qualitative differences from the dependencies presented in Fig. 7 were observed.

The experimental dependencies $R(k)$ and $R(\varphi_0)$ are shown in Fig. 8. They are qualitatively

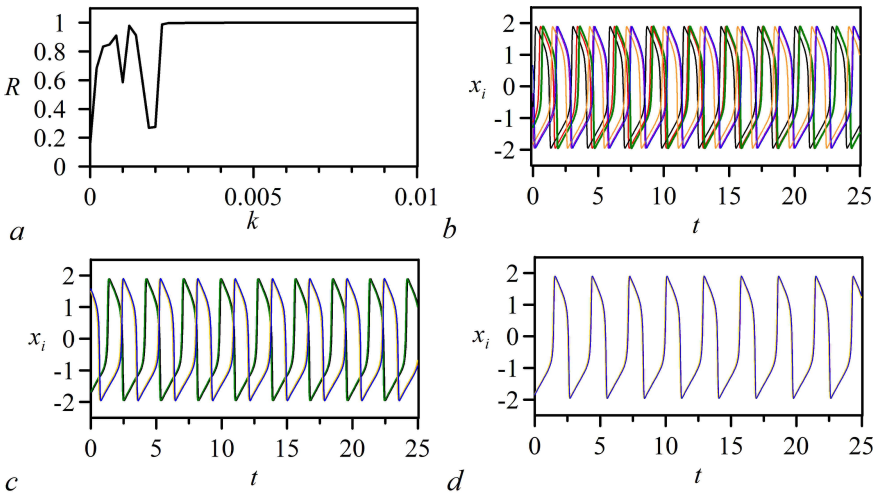

Fig 6. Dependence $R(k)$ at $\varphi_0 = -0.5$ and $x_i(0) = 0.2$, $y_i(0) = 0.1$ for $N = 6$ (*a*) and temporal realizations of $x_i(t)$ at $k = 0.0001$ (*b*), $k = 0.002$ (*c*) and $k = 0.003$ (*d*) (color online)

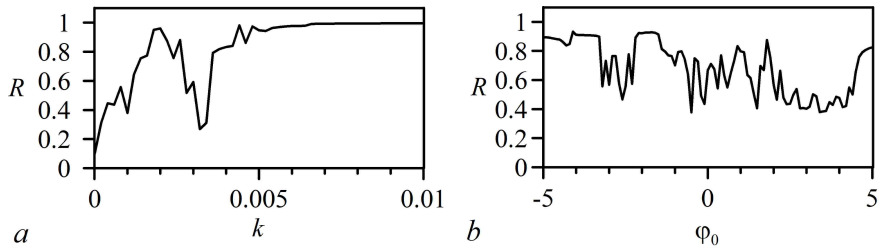

Fig 7. *a* — Dependence $R(k)$ at $\varphi_0 = -0.5$ and $x_i(0) = 0.2$, $y_i(0) = 0.1$ for $N = 10$. *b* — Dependence $R(\varphi_0)$ at $k = 0.001$ for $N = 10$

similar to the analogous dependencies in Fig. 7 obtained in numerical simulation.

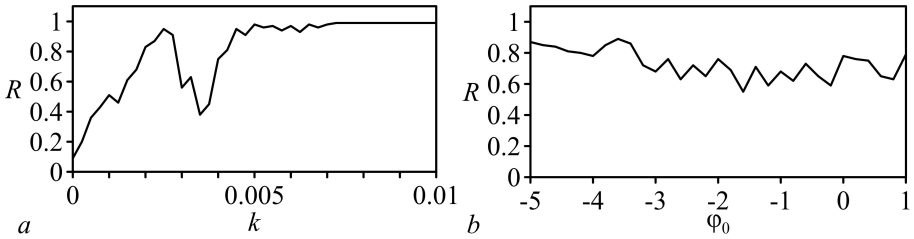

Fig 8. Experimental dependence $R(k)$ at $\varphi_0 = -0.5$ for $N = 10$. *b* — Experimental dependence $R(\varphi_0)$ at $k = 0.001$ for $N = 10$

Conclusion

We have carried out a numerical and experimental study of synchronization in a ring of memristively coupled non-identical FitzHugh-Nagumo oscillators. It is shown that with memristive coupling of FitzHugh-Nagumo oscillators, their synchronization depends not only on the value of the coupling coefficient, but also on the initial states of the oscillators themselves and the variables responsible for the memristive coupling. The features of synchronization depending on the number of oscillators in the ring are studied. It is found that the dependence of synchronization on the initial states of the oscillators is more pronounced in a ring with a small number of elements. Moreover, the more the initial states of different oscillators differ, the more difficult it is to achieve complete synchronization of all oscillators in the ensemble. For complete synchronization of non-identical oscillators in a ring with a large number of elements, higher values of the coupling coefficient are required than for a ring with a small number of elements. It is shown that, unlike the case of diffusive coupling of oscillators, with memristive coupling, with an increase in the coupling strength of oscillators, the destruction of the regime of fully synchronous in-phase oscillations can be observed. Instead, a regime of out-of-phase oscillations arises. The results obtained in the radiophysical experiment for a ring of analog FitzHugh-Nagumo generators connected by a digitally implemented memristive coupling are in good agreement with the results of numerical modeling.

The task of synchronization control in ensembles of neural oscillators is relevant for many applications. Moreover, synchronization can play a positive role, but it can also be undesirable. For example, in robotics, when developing central pattern generators, it is important to ensure in-phase synchronization of ensemble elements in a wide range of control parameters. Excessive synchronization of brain neurons can cause such neurological diseases as epilepsy, schizophrenia, and Parkinson's disease. Therefore, both the problem of in-phase synchronization of oscillations in an ensemble of coupled neuron-like oscillators and the problem of destruction of the synchronization

mode are of great interest.

The solution of these problems can be helped by using memristive coupling of oscillators. Complete (in-phase) synchronization in an ensemble of memristively coupled oscillators occurs at lower values of the constant coupling coefficient k than in an ensemble of diffusion-coupled oscillators. That is, with the help of memristive coupling it is easier to synchronize neuron-like oscillators. On the other hand, without changing the coupling strength k, it is possible to achieve the destruction of in-phase oscillations of oscillators by changing the initial conditions of the dynamic variables.

References

1. Yamazaki K, Vo-Ho V-K, Bulsara D, Le N. Spiking neural networks and their applications: A review. Brain Sciences. 2022;12(7):863. DOI: 10.3390/brainsci12070863.
2. Quiroga RQ, Panzeri S. Principles of Neural Coding. Boca Raton: CRC Press; 2013. 664 p.
3. Kasabov N. Evolving Connectionist Systems: The Knowledge Engineering Approach. London: Springer; 2007. 451 p. DOI: 10.1007/978-1-84628-347-5.
4. Lobov S, Mironov V, Kastalskiy I, Kazantsev V. A spiking neural network in sEMG fea-ture extraction. Sensors. 2015;15(11):27894–27904. DOI: 10.3390/s151127894.
5. *Lobov SA, Chernyshov AV, Krilova NP, Shamshin MO, Kazantsev VB.* Competitive learning in a spiking neural network: Towards an intelligent pattern classifier // Sensors. 2000;20(2): 500. DOI: 10.3390/s20020500.
6. Virgilio GCD, Sossa AJH, Antelis JM, Falcón LE. Spiking Neural Networks applied to the classification of motor tasks in EEG signals. Neural Netw. 2020;122:130–143. DOI: 10.1016/j.neunet.2019.09.037.
7. Andreev AV, Ivanchenko MV, Pisarchik AN, Hramov AE. Stimulus classification using chimera-like states in a spiking neural network. Chaos, Solitons & Fractals. 2020;139:110061. DOI: 10.1016/j.chaos.2020.110061.
8. Navrotskaya EV, Kulminskiy DD, Ponomarenko VI, Prokhorov MD. Estimation of impulse action parameters using a network of neuronlike oscillators. Izvestiya VUZ. Applied Nonlinear Dynamics. 2022;30(4):495–512. DOI: 10.18500/0869-6632-2022-30-4-495-512.
9. Hossain MS, Muhammad G. Emotion recognition using deep learning approach from audio–visual emotional big data. Information Fusion. 2019;49:69–78. DOI: 10.1016/j.inffus.2018.09.008.
10. Yu D, Deng L. Automatic Speech Recognition: A Deep Learning Approach. London: Springer; 2015. 321 p. DOI: 10.1007/978-1-4471-5779-3.
11. Bing Z, Meschede C, Röhrbein F, Huang K, Knoll AC. A survey of robotics control based on learning-inspired spiking neural networks. Frontiers in Neurorobotics. 2018;12:35. DOI: 10.3389/fnbot.2018.00035.
12. Wang X, Hou Z-G, Lv F, Tan M, Wang Y. Mobile robots' modular navigation controller using spiking neural networks. Neurocomputing. 2014;134:230–238. DOI: 10.1016/j.neucom.2013.07.055.
13. Chou T-S, Bucci LD, Krichmar JL. Learning touch preferences with a tactile robot using dopamine modulated STDP in a model of insular cortex. Frontiers in Neurorobotics. 2015;9:6. DOI: 10.3389/fnbot.2015.00006.
14. Lobov SA, Mikhaylov AN, Shamshin M, Makarov VA, Kazantsev VB. Spatial properties of STDP in a self-learning spiking neural network enable controlling a mobile robot. Frontiers in Neuroscience. 2020;14:88. DOI: 10.3389/fnins.2020.00088.
15. Yi Z, Lian J, Liu Q, Zhu H, Liang D, Liu J. Learning rules in spiking neural networks: A survey. Neurocomputing. 2023;531:163–179. DOI: 10.1016/j.neucom.2023.02.026.

16. Dmitrichev AS, Kasatkin DV, Klinshov VV, Kirillov SY, Maslennikov OV, Shchapin DS, Nekorkin VI. Nonlinear dynamical models of neurons: Review. Izvestiya VUZ. Applied Nonlinear Dynamics. 2018;26(4):5–58. DOI: 10.18500/0869-6632-2018-26-4-5-58.
17. Shepelev IA, Slepnev AV, Vadivasova TE. Different synchronization characteristics of distinct types of traveling waves in a model of active medium with periodic boundary conditions. Communications in Nonlinear Science and Numerical Simulation. 2016;38:206–217. DOI: 10.1016/j.cnsns.2016.02.020.
18. Shepelev IA, Vadivasova TE, Bukh AV, Strelkova GI, Anishchenko VS. New type of chimera structures in a ring of bistable FitzHugh–Nagumo oscillators with nonlocal interaction. Physics Letters A. 2017;381(16):1398–1404. DOI: 10.1016/j.physleta.2017.02.034.
19. Shepelev IA, Shamshin DV, Strelkova GI, Vadivasova TE. Bifurcations of spatiotemporal structures in a medium of FitzHugh–Nagumo neurons with diffusive coupling. Chaos, Solitons & Fractals. 2017;104:153–160. DOI: 10.1016/j.chaos.2017.08.009.
20. Plotnikov SA, Fradkov AL. On synchronization in heterogeneous FitzHugh–Nagumo networks. Chaos, Solitons & Fractals. 2019;121:85–91. DOI: 10.1016/j.chaos.2019.02.006.
21. Kulminskiy DD, Ponomarenko VI, Prokhorov MD, Hramov AE. Synchronization in ensembles of delay-coupled nonidentical neuronlike oscillators. Nonlinear Dynamics. 2019;98(1):735–748. DOI: 10.1007/s11071-019-05224-x.
22. Plotnikov SA, Lehnert J, Fradkov AL, Schöll E. Adaptive control of synchronization in delay-coupled heterogeneous networks of FitzHugh–Nagumo nodes. Int. J. Bifurc. Chaos. 2016;26(4):1650058. DOI: 10.1142/S0218127416500589.
23. Kurbako AV, Ponomarenko VI, Prokhorov MD. Adaptive control of non-synchronous oscillations in a network of identical electronic neuron-like generators. Tech. Phys. Lett. 2022;48(10):38–41. DOI: 10.21883/TPL.2022.10.54796.19328.
24. Korneev IA, Slepnev AV, Semenov VV, Vadivasova TE. Wave processes in a ring of memristively coupled self-excited oscillators. Izvestiya VUZ. Applied Nonlinear Dynamics. 2020;28(3):324–340 (in Russian). DOI: 10.18500/0869-6632-2020-28-3-324-340.
25. Wang C, Lv M, Alsaedi A, Ma J. Synchronization stability and pattern selection in a memristive neuronal network. Chaos. 2017;27(11):113108. DOI: 10.1063/1.5004234.
26. Xu F, Zhang J, Jin M, Huang S, Fang T. Chimera states and synchronization behavior in multilayer memristive neural networks. Nonlinear Dynamics. 2018;94(2):775–783. DOI: 10.1007/s11071-018-4393-9.
27. Usha K, Subha PA. Collective dynamics and energy aspects of star-coupled Hindmarsh–Rose neuron model with electrical, chemical and field couplings. Nonlinear Dynamics. 2019;96(3):2115–2124. DOI: 10.1007/s11071-019-04909-7.
28. Bao H, Zhang Y, Liu W, Bao B. Memristor synapse-coupled memristive neuron network: synchronization transition and occurrence of chimera. Nonlinear Dynamics. 2020;100(1):937–950. DOI: 10.1007/s11071-020-05529-2.
29. Korneev IA, Semenov VV, Slepnev AV, Vadivasova TE. The impact of memristive coupling initial states on travelling waves in an ensemble of the FitzHugh–Nagumo oscillators. Chaos, Solitons & Fractals. 2021;147:110923. DOI: 10.1016/j.chaos.2021.110923.
30. Xu Y, Jia Y, Ma J, Alsaedi A, Ahmad B. Synchronization between neurons coupled by memristor. Chaos, Solitons & Fractals. 2017;104:435–442. DOI: 10.1016/j.chaos.2017.09.002.
31. Gerasimova SA, Mikhaylov AN, Belov AI, Korolev DS, Gorshkov ON, Kazantsev VB. Simulation of synaptic coupling of neuron-like generators via a memristive device. Tech. Phys. 2017;62(8):1259–1265. DOI: 10.1134/S1063784217080102.
32. Chua L. Memristor-The missing circuit element. IEEE Transactions on Circuit Theory. 1971;18(5):507–519. DOI: 10.1109/TCT.1971.1083337.

33. Chua LO, Kang SM. Memristive devices and systems. Proceedings of the IEEE. 1976;64(2): 209–223. DOI: 10.1109/PROC.1976.10092.
34. Strukov DB, Snider GS, Stewart DR, Williams RS. The missing memristor found. Nature. 2008;453(7191):80–83. DOI: 10.1038/nature06932.
35. Patterson GA, Fierens PI, García AA, Grosz DF. Numerical and experimental study of stochastic resistive switching. Phys. Rev. E. 2013;87(1):012128. DOI: 10.1103/PhysRevE.87.012128.